Space optical remote sensor image motion velocity vector computational modeling, error budget and synthesis

Jiaqi Wang (王家骐), Ping Yu (于 平), Changxiang Yan (颜昌翔), Jianyue Ren (任建岳), and Bin He (何 斌)

Changchun Institute of Optics, Fine Mechanics and Physics, Chinese Academy of Sciences, Changchun 130033

Received September 27, 2004

For space optical remote sensor (SORS) with either film or time delay and integrate charge coupled device (TDI-CCD) imaging, in order to achieve higher resolution it requires more accurate real-time image motion compensation. This primarily depends on real-time computation of the image motion velocity vector (IMVV) and error budget and synthesis on related parameters. An effective modeling scheme is introduced and the derivation of IMVV equation, error budget and synthesis by Monte-Carlo method are presented in detail. This total solution was applied to SORS system test on orbit and has been confirmed to be very accurate based on the resolution, transfer function at Nyquist frequency, signal-to-noise ratio and average gray scale of the captured images.

OCIS codes: 080.2720, 110.5200, 120.5240, 280.0280, 350.6090.

For space optical remote sensor (SORS), real-time image motion compensation has become the key technology to meet the ever-increasing image resolution requirement. This primarily depends on real time computation of image motion velocity vector (IMVV) and error budget analysis and synthesis on related parameters. In this paper, beginning with the definition of 7 coordinates from object to image plane and 14 linear coordinate transformations, the IMVV equation is derived based on the image plane position and velocity equations with total of 15 parameters. Then the error budget is given for 11 parameters which affect IMVV. Finally error synthesis is carried out using Monte-Carlo method.

There are 7 coordinates involved in the coordinate transformation from object to image plane on SORS. Each coordinate is defined as follows (all right-handed, as Fig. 1):

a) Geocentric inertial coordinates $I(I_1, I_2, I_3)$
The origin is at geocenter. I_2 points to north pole. I_3 is along the intersection of spacecraft orbital plane and equator plane. I_1 is perpendicular to I_2 and I_3. This coordinates are in inertial space.

b) Geodetic coordinates $E(E_1, E_2, E_3)$
The origin is at geocenter. E_2 points to north pole as I_2. This coordinates rotate counter-clockwise at angular velocity ω around E_2.

c) Spacecraft orbital coordinates $B(B_1, B_2, B_3)$
The origin is on the orbit. B_1 is along the orbital forward direction. B_3 points to sky dome, which also passes the origin of I coordinates. B_1 and B_3 are in the orbital plane and B_2 is perpendicular to it. B coordinates orbit at angular velocity of Ω in I coordinates.

d) Geographical coordinates $G(G_1, G_2, G_3)$
It is the axial translation of B coordinates by $-(H-h)$ along B_3, where $H-h$ is the actual spacecraft height measured from object.

e) Spacecraft coordinates $S(S_1, S_2, S_3)$
The origin is the same as that of B coordinates. S coincides with B when the spacecraft is not in positional movement. The three spacecraft axial positions of ϕ, θ, and Ψ mean that of s coordinates in B coordinates.

f) SORS coordinates $C(C_1, C_2, C_3)$
The origin is the principal point of SORS object lens. It is the scale-down of S by $f/(H-h)$ provided that the SORS is assembled with minor or no error.

g) Image plane coordinates $P(P_1, P_2, P_3)$
The origin is centered at the image plane. It is the axial translation of C coordinates by f, where f is the focal length of the SORS object lens. P_1 and P_2 are in the image plane.

To find the relationship between the earth object in G coordinates and image in P coordinates, 14 linear coordinate transformations are performed. The detailed coordinate transformation operations are given as

$$G-\text{Geography} \xrightarrow[\text{Rotate } (G_2)-\gamma_0 \\ \text{Rotate } (G_3)-i_0]{\text{Shift } (G_3)-(R+h)} E-\text{Earth} \xrightarrow[-\omega t]{\text{Rotate } (E_2)} I-\text{Inertial earth} \xrightarrow[\text{Rotate } (I_2)\gamma_0+\Omega t \\ \text{Rotate } (I_3)(R+H)]{\text{Rotate } (I_3)-i_0}$$

$$B-\text{Orbit} \xrightarrow[\text{Rotate } (B_3)\theta_0+\dot{\theta}t \\ \text{Rotate } (B_1)\phi_0+\dot{\phi}t]{\text{Rotate } (B_3)\Psi_0+\dot{\Psi}t} S-\text{Spacecraft} \xrightarrow{\text{Scale } (f/H-h)} C-\text{Remote sensor} \xrightarrow{\text{Scale } (G_3)f} P-\text{Image plane}$$

To clarify, we use abbreviations in the form of $F[X, Y]$ to describe the operations. F is one of the three operations, which are translation (TR), rotation (RT), and scale-down (SC). X is the axis of the related operation. Y is the amount of the operation.

Following the procedures shown in Fig. 1, the equation for transformation from G to P coordinates can be written as

$$P=\begin{bmatrix}P_1\\P_2\\P_3\\1\end{bmatrix}=\begin{bmatrix}-f/H-h&0&0&0\\0&-f/H-h&0&0\\0&0&f/H-h&-f\\0&0&0&1\end{bmatrix}\begin{bmatrix}1&0&0&0\\0&\cos\varphi&\sin\varphi&0\\0&-\sin\varphi&\cos\varphi&0\\0&0&0&1\end{bmatrix}\begin{bmatrix}\cos\theta&0&-\sin\theta&0\\0&1&0&0\\\sin\theta&0&\cos\theta&0\\0&0&0&1\end{bmatrix}$$

$$\begin{bmatrix}\cos\Psi&\sin\Psi&0&0\\-\sin\Psi&\cos\Psi&0&0\\0&0&1&0\\0&0&0&1\end{bmatrix}\begin{bmatrix}1&0&0&0\\0&1&0&0\\0&0&1&-(R+H)\\0&0&0&1\end{bmatrix}\begin{bmatrix}\cos\gamma&0&-\sin\gamma&0\\0&1&0&0\\\sin\gamma&0&\cos\gamma&0\\0&0&0&1\end{bmatrix}\begin{bmatrix}\cos i_0&-\sin i_0&0&0\\\sin i_0&\cos i_0&0&0\\0&0&1&0\\0&0&0&1\end{bmatrix}$$

$$\begin{bmatrix}\cos\omega t&0&\sin\omega t&0\\0&1&0&0\\-\sin\omega t&0&\cos\omega t&0\\0&0&0&1\end{bmatrix}\begin{bmatrix}\cos i_0&\sin i_0&0&0\\-\sin i_0&\cos i_0&0&0\\0&0&1&0\\0&0&0&1\end{bmatrix}\begin{bmatrix}\cos\gamma_0&0&\sin\gamma_0&0\\0&1&0&0\\-\sin\gamma_0&0&\cos\gamma_0&0\\0&0&0&1\end{bmatrix}\begin{bmatrix}1&0&0&0\\0&1&0&0\\0&0&1&(R+H)\\0&0&0&1\end{bmatrix}\begin{bmatrix}G_1\\G_2\\0\\1\end{bmatrix}. \tag{1}$$

To be more concise, we replace 'sin' and 'cos' with 'S' and 'C'.
Set $t=0$, G coordinate can be calculated from

$$\begin{cases}G_1=(\frac{H-h}{f})(\frac{P_2-f\mathrm{S}\varphi_0\mathrm{C}\theta_0}{\mathrm{C}\varphi_0\mathrm{C}\Psi_0+\mathrm{S}\varphi_0\mathrm{S}\theta_0\mathrm{S}\Psi_0}-\frac{P_1+f\mathrm{S}\theta_0}{\mathrm{C}\theta_0\mathrm{S}\Psi_0})\Big/(\frac{\mathrm{C}\Psi_0}{\mathrm{S}\Psi_0}-\frac{\mathrm{S}\varphi_0\mathrm{S}\theta_0\mathrm{C}\Psi_0-\mathrm{C}\varphi_0\mathrm{S}\Psi_0}{\mathrm{C}\varphi_0\mathrm{C}\Psi_0+\mathrm{S}\varphi_0\mathrm{S}\theta_0\mathrm{S}\Psi_0})\\ G_2=(\frac{H-h}{f})(\frac{P_2-f\mathrm{S}\varphi_0\mathrm{C}\theta_0}{\mathrm{S}\varphi_0\mathrm{S}\theta_0\mathrm{C}\Psi_0-\mathrm{C}\varphi_0\mathrm{S}\Psi_0}-\frac{P_1+f\mathrm{S}\theta_0}{\mathrm{C}\theta_0\mathrm{C}\Psi_0})\Big/(\frac{\mathrm{S}\Psi_0}{\mathrm{C}\Psi_0}-\frac{\mathrm{C}\varphi_0\mathrm{C}\Psi_0+\mathrm{S}\varphi_0\mathrm{S}\theta_0\mathrm{S}\Psi_0}{\mathrm{S}\varphi_0\mathrm{S}\theta_0\mathrm{C}\Psi_0-\mathrm{C}\varphi_0\mathrm{S}\Psi_0})\end{cases}. \tag{2}$$

By differentiating both sides of Eq. (1) with t and set $t=0$, the image motion equation is obtained as

$$\left.\frac{\mathrm{d}P}{\mathrm{d}t}\right|_{t=0}=\begin{bmatrix}\mathrm{d}P_1/\mathrm{d}t\\\mathrm{d}P_2/\mathrm{d}t\\\mathrm{d}P_3/\mathrm{d}t\\0\end{bmatrix}_{t=0}=\begin{bmatrix}V_{P_1}\\V_{P_2}\\V_{P_3}\\0\end{bmatrix},$$

$$\begin{aligned}V_{P_1}&=\mathrm{d}P_1/\mathrm{d}t|_{t=0}=\\&\frac{f}{H-h}[\Omega(R+h)-\omega(R+h)\mathrm{C}i_0-G_2\omega\mathrm{S}i_0\mathrm{S}\gamma_0]\mathrm{C}\theta_0\mathrm{C}\Psi_0\\&-\frac{f}{H-h}[\omega(R+h)\mathrm{S}i_0\mathrm{C}\gamma_0-G_1\omega\mathrm{S}i_0\mathrm{S}\gamma_0]\mathrm{C}\theta_0\mathrm{S}\Psi_0\\&+\frac{f}{H-h}[G_1\Omega-G_1\omega\mathrm{C}i_0-G_2\omega\mathrm{S}i_0\mathrm{C}\gamma_0]\mathrm{S}\theta_0\\&+\frac{G_1f}{H-h}(\dot\theta\mathrm{S}\theta_0\mathrm{C}\Psi_0+\dot\Psi\mathrm{C}\theta_0\mathrm{S}\Psi_0)\\&+\frac{G_2f}{H-h}(\dot\theta\mathrm{S}\theta_0\mathrm{S}\Psi_0-\dot\Psi\mathrm{C}\theta_0\mathrm{C}\Psi_0)-f\dot\theta\mathrm{C}\theta_0,\end{aligned} \tag{3}$$

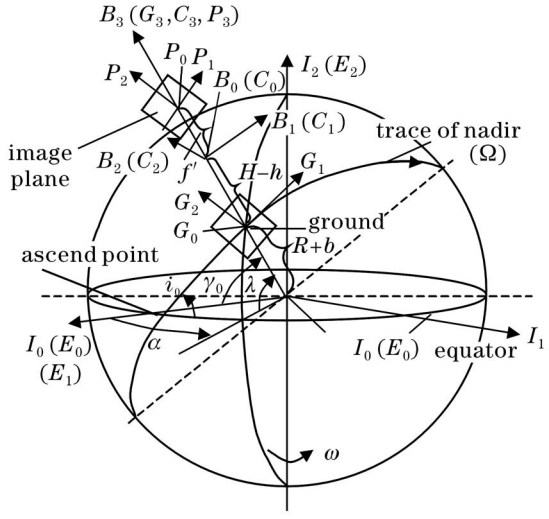

Fig. 1. Geography relation of optical remote sensor when imaging nadir.

$$\begin{aligned}V_{P_2}&=\mathrm{d}P_2/\mathrm{d}t|_{t=0}=\\&\frac{f}{H-h}[\Omega(R+h)-\omega(R+h)\mathrm{C}i_0-G_2\omega\mathrm{S}i_0\mathrm{S}\gamma_0]\\&\times(-\mathrm{C}\varphi_0\mathrm{S}\Psi_0+\mathrm{S}\varphi_0\mathrm{S}\theta_0\mathrm{C}\Psi_0)\\&-\frac{f}{H-h}[\omega(R+h)\mathrm{S}i_0\mathrm{C}\gamma_0-G_1\omega\mathrm{S}i_0\mathrm{S}\gamma_0]\\&\times(\mathrm{C}\varphi_0\mathrm{C}\Psi_0+\mathrm{S}\varphi_0\mathrm{S}\theta_0\mathrm{S}\Psi_0)\\&-\frac{f}{H-h}(G_1\Omega-G_1\omega\mathrm{C}i_0-G_2\omega\mathrm{S}i_0\mathrm{C}\gamma_0)\mathrm{S}\varphi_0\mathrm{C}\theta_0\\&-\frac{G_1f}{H-h}[\dot\varphi(\mathrm{S}\varphi_0\mathrm{S}\Psi_0+\mathrm{C}\varphi_0\mathrm{S}\theta_0\mathrm{C}\Psi_0)+\dot\theta\mathrm{S}\varphi_0\mathrm{C}\theta_0\mathrm{C}\Psi_0\\&-\dot\Psi(\mathrm{C}\varphi_0\mathrm{C}\Psi_0+\mathrm{S}\varphi_0\mathrm{S}\theta_0\mathrm{S}\Psi_0)]\\&+\frac{G_2f}{H-h}[\dot\varphi(\mathrm{S}\varphi_0\mathrm{C}\Psi_0-\mathrm{C}\varphi_0\mathrm{S}\theta_0\mathrm{S}\Psi_0)-\dot\theta\mathrm{S}\varphi_0\mathrm{C}\theta_0\mathrm{S}\Psi_0\\&+\dot\Psi(\mathrm{C}\varphi_0\mathrm{S}\Psi_0-\mathrm{S}\varphi_0\mathrm{S}\theta_0\mathrm{C}\Psi_0)]+f(\dot\varphi\mathrm{C}\varphi_0\mathrm{C}\theta_0-\dot\theta\mathrm{S}\varphi_0\mathrm{S}\theta_0).\end{aligned} \tag{4}$$

Finally, the absolute value of image motion velocity principal vector and yaw angle are given by

$$V_P = \sqrt{V_{P_1}^2 + V_{P_2}^2}, \tag{5}$$

$$\beta_P = \arctan(V_{P_2}/V_{P_1}). \tag{6}$$

In the above equations, the parameters are defined as follows. R — earth radius relative to geocenter (km); H — spacecraft orbital height measured from the object (km); h — object height (km); $H-h$ — actual height of spacecraft measured from the object (km); $R+H$ — spacecraft orbital height relative to geocenter (km); $R+h$ — geocentric distance of the object (km); i_0 — orbit obliquity (angle between orbital plane and earth equator plane); ω — earth rotation angular speed 7.2921×10^{-5} s^{-1}; Ω — spacecraft orbital angular speed relative to geocenter (s^{-1}) during imaging; V_s — spacecraft moving speed along horizontal direction during imaging. $V_s = \Omega(R+H)$ (km/s); ψ_0, θ_0, φ_0 — yaw, pitch, and roll angle of S coordinates relative to G coordinates during imaging; $\dot{\psi}$, $\dot{\theta}$, $\dot{\varphi}$ — yaw, pitch, and roll angular speed of S coordinates relative to G coordinates; $\psi_{\max}$, $\theta_{\max}$, $\varphi_{\max}$ — the maximum of yaw, pitch and roll angle. $|\psi_{\max}| = 0.7°$, $|\theta_{\max}| = |\varphi_{\max}| = 0.5°$; $\dot{\psi}_{\max}$, $\dot{\theta}_{\max}$, $\dot{\varphi}_{\max}$ — the maximum of yaw, pitch and roll angular speed. $\left|\dot{\psi}_{\max}\right| = \left|\dot{\theta}_{\max}\right| = |\dot{\varphi}_{\max}| = 0.02°$/s; γ_0 — $\gamma_0 = \arcsin(\sin\lambda/\sin i_0)$; f — focal length of SORS object lens (mm); V_{P_1}, V_{P_2} — IMVV projected value along the P_1, P_2 axis (mm/s); V_P — absolute value of IMVV; β_P — yaw angle, that is, the angle between IMVV and P_1 axis.

Among the parameters listed above, 11 variables need to be considered for error budget. Based on the requirement of the TDI-CCD with 96 TDI stages, or the film with 0.01 s exposure time, the standard deviation allowance for each variable is listed in Table 1.

Now that standard deviations for the 11 random variables are given in Table 1, standard deviation of V_{P_1}, V_{P_2}, V_P and β_P can then be theoretically derived by total differentiation of Eqs. (3)—(6). However, it is extremely complicated. Therefore, we did error synthesis numerically by Monte-Carlo method. The detailed synthesis procedures are listed as follows:

a) As shown in Table 2, sequence $S_{i,j}$ with 17 pseudo-random numbers is created for the 11 random variables and 6 position initial value, $i = 1, 2, \cdots, n$ (n is the total sampling points, which is a big number); $j = 1, 2, \cdots, m$ ($m = 17$, which means 17 pseudo-random numbers).

Table 1. Variables Standard Deviation Allowance

Variables	Standard Deviation Allowance
σ_{V_s} (km/s)	0.01
σ_{H-h} (km)	0.1
σ_{R+h} (km)	0.05
σ_λ (km)	3
$\sigma_\psi = \sigma_\theta = \sigma_\varphi$ (deg.)	0.05
$\sigma_{\dot{\psi}} = \sigma_{\dot{\theta}} = \sigma_{\dot{\varphi}}$ (deg./s)	0.002
σ_f (mm)	1.35

Table 2. Random Error Computation

Index i, j	Uniform Distribution Random Matrix $S_{i,j}$	Normal Distribution Random Matrix $T_{i,j}$	Random Error
1	$S_{i,1}$		$\phi_0 = 2(S_{i,1} - 0.5)\phi_{\max}$
2	$S_{i,2}$		$\theta_0 = 2(S_{i,2} - 0.5)\theta_{\max}$
3	$S_{i,3}$		$\psi_0 = 2(S_{i,3} - 0.5)\psi_{\max}$
4	$S_{i,4}$		$\dot{\phi} = 2(S_{i,1} - 0.5)\dot{\phi}_{\max}$
5	$S_{i,5}$		$\dot{\theta} = 2(S_{i,2} - 0.5)\dot{\theta}_{\max}$
6	$S_{i,6}$		$\dot{\psi} = 2(S_{i,3} - 0.5)\dot{\psi}_{\max}$
7		$T_{i,7}$	$\Delta V_s = T_{i,7} \cdot \sigma_{V_s}$
8		$T_{i,8}$	$\Delta(H-h) = T_{i,8} \cdot \sigma_{H-h}$
9		$T_{i,9}$	$\Delta(R+h) = T_{i,9} \cdot \sigma_{R+h}$
10		$T_{i,10}$	$\Delta\lambda = T_{i,10} \cdot \sigma_\lambda$
11		$T_{i,11}$	$\Delta f = T_{i,11} \cdot \sigma_f$
12		$T_{i,12}$	$\Delta\phi = T_{i,12} \cdot \sigma_\phi$
13		$T_{i,13}$	$\Delta\theta = T_{i,13} \cdot \sigma_\theta$
14		$T_{i,14}$	$\Delta\psi = T_{i,14} \cdot \sigma_\psi$
15		$T_{i,15}$	$\Delta\dot{\phi} = T_{i,15} \cdot \sigma_{\dot{\phi}}$
16		$T_{i,16}$	$\Delta\dot{\theta} = T_{i,16} \cdot \sigma_{\dot{\theta}}$
17		$T_{i,17}$	$\Delta\dot{\psi} = T_{i,17} \cdot \sigma_{\dot{\psi}}$

Need to be mentioned is that, i_0, ω are constants, also the error of γ_0 has been taken into account in σ_λ.

Among the 17 random variables, φ_0, θ_0, ψ_0, $\dot{\varphi}$, $\dot{\theta}$ and $\dot{\psi}$ are uniform distribution, which create random matrices S_{ij}, where $i = 1, 2, \cdots, n$, $j = 1, 2, \cdots, 6$. The rest variables are norm distribution, which create random matrices T_{ij}, where $i = 1, 2, \cdots, n$, $j = 7, 8, \cdots, 17$.

b) After setting $i = 1$ to obtain $\varphi_{0(i=1)}$, $\theta_{0(i=1)}$, $\psi_{0(i=1)}$, $\dot{\varphi}_{0(i=1)}$, $\dot{\theta}_{0(i=1)}$, and $\dot{\psi}_{0(i=1)}$ based on Table 2 and using Eqs. (3) and (4) to calculate $V_{S(i=1)}$, $(H-h)_{(i=1)}$, $(R+h)_{(i=1)}$, and $f_{(i=1)}$ at specific time t, all these values together with i_0, γ_0, and ω are plugged into Eqs. (3)—(6) to get $V_{P(i=1)}$ and $\beta_{P(i=1)}$ for the fist sampling point.

c) Similar to procedure b), all of the following terms $(\varphi_{0(i=1)} + \Delta\varphi_{(i=1)})$, $(\theta_{0(i=1)} + \Delta\theta_{(i=1)})$, $(\psi_{0(i=1)} + \Delta\psi_{(i=1)})$, $(\dot{\varphi}_{0(i=1)} + \Delta\dot{\varphi}_{(i=1)})$, $\dot{\theta}_{0(i=1)} + \Delta\dot{\theta}_{(i=1)})$, $(\dot{\psi}_{0(i=1)} + \Delta\dot{\psi}_{(i=1)})$, $(V_{s(i=1)} + \Delta V_{s(i=1)})$, $[(H-h)_{(i=1)} + \Delta(H-h)_{(i=1)}]$, $[(R+h)_{(i=1)} + \Delta(R+h)_{(i=1)}]$, $(f_{(i=1)} + \Delta f_{(i=1)})$ and $(\gamma_{0(i=1)} + \Delta\gamma_{0(i=1)})$ are calculated and plugged together with i_0 and ω into Eqs. (3)—(6) to get $(V_P + \Delta V_P)_{(i=1)}$ and $(\beta_P + \Delta\beta_P)_{(i=1)}$.

Therefore, $\Delta V_{P(i=1)}$ and $\Delta\beta_{P(i=1)}$ are given by

$$\Delta V_{P(i=1)} = (V_P + \Delta V_P)_{(i=1)} - V_{P(i=1)}, \tag{7}$$

$$\Delta\beta_{P(i=1)} = (\beta_P + \Delta\beta_P)_{(i=1)} - \beta_{P(i=1)}. \tag{8}$$

d) Based on the shooting period, $\gamma_{0(i=2)}$ is obtained by specific increment to $\gamma_{0(i=1)}$. Then procedures b) and c) are repeated by using 17 random number created at $i = 2$ and $j = 1, 2, \cdots, 17$, to obtain $\Delta V_{p(i=2)}$ and $\Delta\beta_{P(i=2)}$.

e) All the above procedures are repeated to finally get

Table 3. ΔV_P Probability Distribution

ΔV_P Range (mm/s)	−0.5—−0.4	−0.4—−0.3	−0.3—−0.2	−0.2—−0.1	−0.1—0	0—0.1	0.1—0.2	0.2—0.3	0.3—0.4	0.4—0.5
Probability (%)	0.9	0.89	5.94	16.67	28.5	25.11	16.5	5.4	0.78	0.16

Table 4. ΔV_P Probability Distribution at Various Exposure Time

Exposure Time (s)	1/100	1/150	1/200	1/250	1/300	1/350	1/400
Probability (%)	81.83	91.11	96.9	99.1	99.83	99.89	99.89

Table 5. $\Delta\beta_P$ Probability Distribution

$\Delta\beta_P$ Range (°)	−0.04—−0.03	−0.03—−0.02	−0.02—−0.01	−0.01—0	0—0.01	0.01—0.02	0.02—0.03	0.03—0.04
Probability (%)	0.22	2.22	13	32.33	33.17	16.5	2.33	0.22

two groups of error synthesis sequences for ΔV_P and $\Delta\beta_P$

$$\Delta V_{P(i=1)}, \Delta V_{P(i=2)}, \cdots, \Delta V_{P(i=n)};$$

$$\Delta\beta_{P(i=1)}, \Delta\beta_{P(i=2)}, \cdots, \Delta\beta_{P(i=n)}.$$

The characteristics of error synthesis can be obtained by statistical analysis of the above two groups of sequences. Table 3 shows the probability distribution of ΔV_P. Table 4 shows the probability for $\Delta V_P \cdot t$ within the allowed range of [0, 0.0012 mm] at various exposure time t. Table 5 shows the probability of $\Delta\beta_P$.

In conclusion: a) By using real time computation of IMVV with all the parameters, combined with the Monte-Carlo method for error synthesis and the real time measurement of spacecraft angular velocity, very accurate image motion compensation can be achieved even at somewhat reduced attitude control accuracy of spacecraft. b) This paper only presents the derivation of IMVV while SORS imaging the nadir point. It will be more complicated if SORS has side swing, front swing, or both during imaging. However, IMVV can be derived the same way with unique solution and will not be presented here.

C. Yan is the author to whom the correspondence should be addressed, his e-mail address is yancx@vip.sina.com.

References

1. C. X. Yan and J. Q. Wang, Opt. Precision Eng. (in Chinese) **8,** 203 (2000).
2. Q. X. Sun, Control Eng. (in Chinese) **19,** (5) 1 (1992).
3. Y. M. Zhang, *Applied Optics* (in Chinese) (Mechanism Industry Press, Beijing, 1982).
4. T. Trott, Photogramm. Eng. **26,** 819 (1960).
5. S. Rudoler, O. Hadar, M. Fisher, and N. S. Kopeika, Opt. Eng. **30,** 577 (1991).
6. S. K. Ghosh, Opt. Eng. **24,** 1014 (1985).
7. A. V. Demin and A. A. Dzhamanbaev, Sov. J. Opt. Technol. **62,** 540 (1995).
8. V. A. Toropin, Sov. J. Opt. Technol. **49,** 1 (1982).
9. D. N. Eskov and I. I. Druz, Sov. J. Opt. Technol. **44,** 745 (1977).
10. E. V. Nilov, Sov. J. Opt. Technol. **51,** 221 (1984).